Protective effects of maternal nutritional supplementation with lactoferrin on growth and brain metabolism

Emmanuel Somm[1], Pierre Larvaron[1], Yohan van de Looij[1,2], Audrey Toulotte[1], Alexandra Chatagner[1], Magali Faure[3], Sylviane Métairon[3], Robert Mansourian[3], Frédéric Raymond[3], Rolf Gruetter[2], Bing Wang[3,4], Stéphane V. Sizonenko[1] and Petra S. Hüppi[1]

BACKGROUND: Intrauterine growth restriction (IUGR) is a major risk factor for both perinatal and long-term morbidity. Bovine lactoferrin (bLf) is a major milk glycoprotein considered as a pleiotropic functional nutrient. The impact of maternal supplementation with bLf on IUGR-induced sequelae, including inadequate growth and altered cerebral development, remains unknown.

METHODS: IUGR was induced through maternal dexamethasone infusion (100 µg/kg during last gestational week) in rats. Maternal supplementation with bLf (0.85% in food pellet) was provided during both gestation and lactation. Pups growth was monitored, and pup brain metabolism and gene expression were studied using *in vivo* ^{1}H NMR spectroscopy, quantitative PCR, and microarray in the hippocampus at postnatal day (PND)7.

RESULTS: Maternal bLf supplementation did not change gestational weight but increased the birth body weight of control pup (4%) with no effect on the IUGR pups. Maternal bLf supplementation allowed IUGR pups to recover a normalized weight at PND21 (weaning) improving catch-up growth. Significantly altered levels of brain metabolites (γ-aminobutyric acid, glutamate, N-acetylaspartate, and N-acetylaspartylglutamate) and transcripts (brain-derived neurotrophic factor (BDNF), divalent metal transporter 1 (DMT-1), and glutamate receptors) in IUGR pups were normalized with maternal bLf supplementation.

CONCLUSION: Our data suggest that maternal bLf supplementation is a beneficial nutritional intervention able to revert some of the IUGR-induced sequelae, including brain hippocampal changes.

Intrauterine growth restriction (IUGR) leads to low birth weight, an important predictor of mortality and morbidity in the newborn (1). However, IUGR is not only associated with an increased risk in perinatal mortality but also with a higher prevalence of developing diseases/disabilities later in life (2). This "fetal origin of adult diseases" hypothesis proposes that an impaired intrauterine environment (e.g., deficient in nutrients, oxygen, hormones, or enriched in toxics), leading to abnormal fetal growth and altered tissue development programs the fetus for later chronic diseases in adulthood (2). Although cerebral structures are more preserved than other tissues during deleterious conditions of growth (brain sparing effect), IUGR also compromises brain development and increases the risk for later mental and psychomotor developmental complications, in particular in infants not showing catch-up growth (3). The hippocampus appears to be especially susceptible to the effects of IUGR, as well as in animal models (4) as in the human situation (5). Many experimental models of IUGR, involving maternal restriction in nutrients, exposure to hypoxia/ischemia or limitation in blood supply, have allowed elucidating some mechanisms involved in this deleterious "programming" process. *In utero* exposure to synthetic glucocorticoids is another experimental animal model of IUGR, mimicking maternal stress. Clinically, glucocorticoids are also administered to pregnant women with risk of premature delivery. By enhancing fetal lung maturation, this antenatal treatment presents an immediate benefit for preterm neonate survival but long-term consequences of repeated doses of antenatal glucocorticoid include alterations in growth and brain development (6). Rodent studies also showed that antenatal glucocorticoid exposure predisposes the offspring to early glucose intolerance (7) and disturbed cerebral development (8).

The impact of nutrition in early life on neurodevelopment is a major field of investigation but also a controversial topic due to the complexity of dissociating genetic, environmental, and nutritional influences. However, nutrients naturally present in milk may represent the most appropriate candidates to safely improve early brain development, particularly following adverse prenatal conditions. Lactoferrin (Lf) is a glycoprotein whose highest levels are found in colostrum and in mature milk (9). Lf exhibits pleiotropic biological properties, such as a role in iron homeostasis, in the immune response, in the prevention of tumorigenesis, as well as in anti-inflammatory processes (for review, see ref. 10). Interestingly, this functional nutrient was recently shown to reduce the incidence of late-onset bacterial and fungal sepsis in low-birth-weight neonates (11). Lf is also produced in the brain (12) and its upregulation in the central

The first two authors and the last two authors contributed equally to this work.
[1]Department of Paediatrics, Division of Development and Growth, University of Geneva School of Medicine, Geneva, Switzerland; [2]Laboratory for Functional and Metabolic Imaging, École Polytechnique Fédérale de Lausanne, Lausanne, Switzerland; [3]Nestlé Research Center, Lausanne, Switzerland; [4]School of Animal and Veterinary Science, Charles Sturt University, New South Wales, Australia. Correspondence: Emmanuel Somm (emmanuel.somm@unige.ch)

Received 28 March 2013; accepted 24 June 2013; advance online publication 8 January 2014. doi:10.1038/pr.2013.199

nervous system during neurodegenerative disorders and aging (13) suggests an endogenous neuroprotecting mechanism. Interestingly, exogenous Lf, such as dietary bovine lactoferrin (bLf) ingested with food, is relatively resistant to digestive degradation and is actively transported into the brain (14). Little knowledge about bLf nutritional supplementation during gestation, both on maternal parameters and pup development (including brain), is presently available. The main objective of our study was to assess the effect of maternal bLf nutritional supplementation (0.85% in food pellet) in a dexamethasone-induced IUGR rat model, with special focus on pup growth and early brain metabolism/gene expression in the hippocampus.

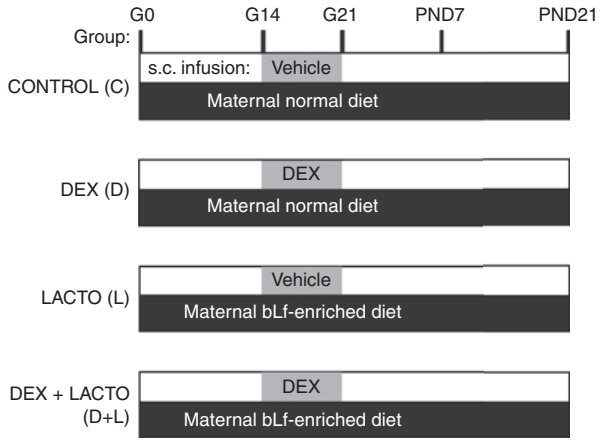

Figure 1. Study experimental groups. The four treatment groups (CONTROL, DEX, LACTO, and DEX+LACTO) of gestating/lactating rats resulting from different subcutaneous (s.c.) infusions (vehicle or dexamethasone (DEX)) and food pellets provided (normal or bLf-enriched). The number refers to gestational or postnatal age in days. bLf, bovine lactoferrin; G, gestational day; PND, postnatal day.

RESULTS

Effect of Nutritional bLf Supplementation on Maternal Weight Gain and Hematological Values During Normal and Dexamethasone (DEX)-Exposed Gestation

To evaluate whether a 0.85% (w/w) bLf nutritional supplementation grossly affects maternal physiology, we monitored weight gain and blood values in gestating dams. Dual gestational subcutaneous DEX infusion and nutritional bLf supplementation resulted in four groups of animals studied in parallel: CONTROL (vehicle infusion/maternal normal diet), DEX (dexamethasone infusion/maternal normal diet), LACTO (vehicle infusion/maternal bLf-enriched diet), and DEX+LACTO (dexamethasone infusion/maternal bLf-enriched diet) (**Figure 1**). Maternal body weight throughout gestation (**Figure 2a**) as well as weight gain during the third

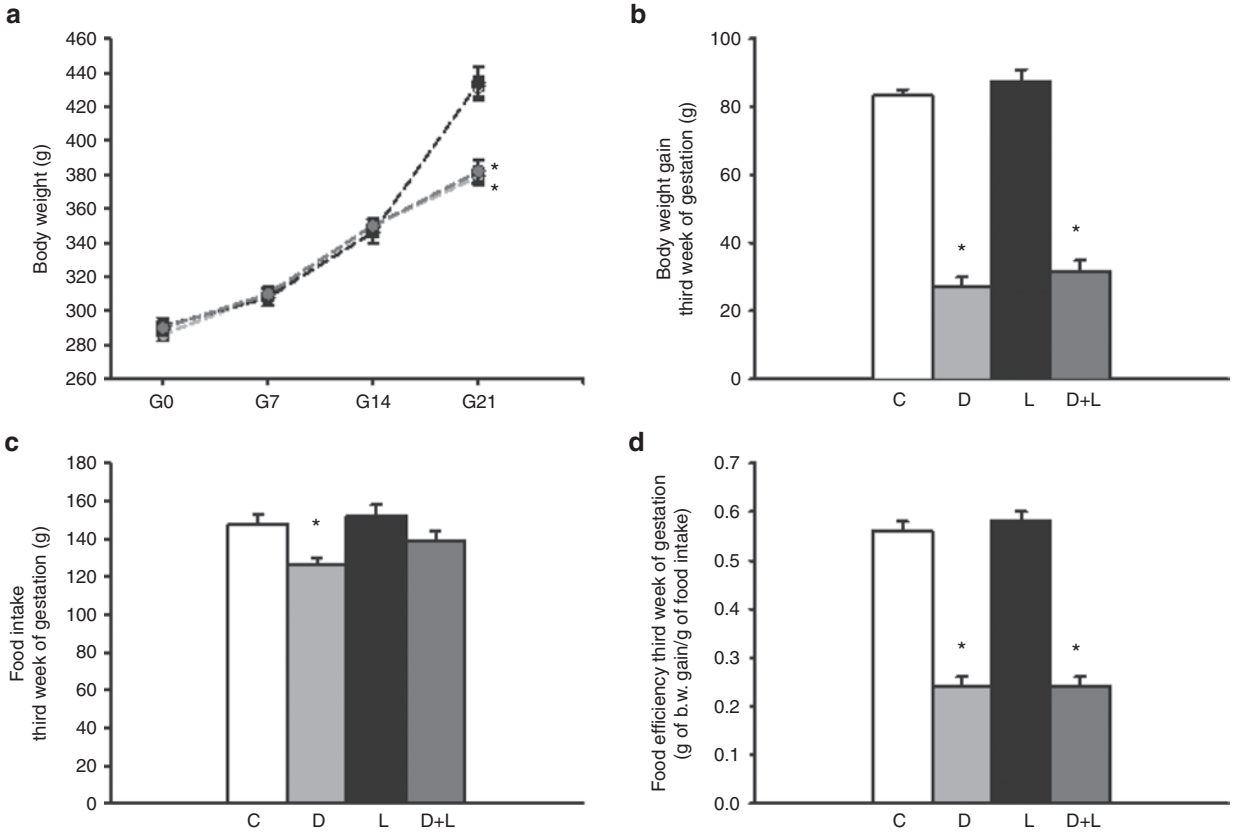

Figure 2. Maternal weight and food intake in dexamethasone (DEX)-exposed and control dams fed with bLf-enriched or normal diet. (**a**) Maternal body weight curve during gestation, *$P < 0.001$ vs. CONTROL. (**b**) Body weight gain, *$P < 0.01$ vs. CONTROL. (**c**) Food intake, *$P < 0.01$ vs. CONTROL. (**d**) Food efficiency, *$P < 0.01$ vs. CONTROL. Panels **b**, **c**, **d** represent data collected during the third week of gestation (G14-21) corresponding to dexamethasone exposure. Results are means ± SEM of $N = 16–21$ gestating dams per group. b.w. body weight; C, CONTROL group (white bar); D, DEX group (light grey bar); D+L, DEX and LACTO group (dark grey bar); L, LACTO group (black bar).

Table 1. Hematological values in gestating rats

	BASAL	CONTROL		DEX		LACTO		DEX+LACTO	
Gestational day	G0	G14	G21	G14	G21	G14	G21	G14	G21
White blood cells ($\times 10^3$/μl)	11.4 ± 0.4	10.0 ± 0.7	10.6 ± 1.3	10.4 ± 0.9	7.2 ± 0.6*,a,b	11.8 ± 0.7	11.1 ± 09	11.1 ± 0.9	7.6 ± 0.5*,b
Lymphocytes ($\times 10^3$/μl)	8.6 ± 0.3	7.3 ± 0.5*	6.1 ± 0.8*	7.3 ± 0.7	1.5 ± 0.3*,a,b	8.4 ± 0.6	6.3 ± 0.6*,b	8.0 ± 1.0	1.9 ± 0.4*,b
Red blood cells ($\times 10^6$/μl)	7.1 ± 0.1	6.8 ± 0.2	5.6 ± 0.4*,b	6.7 ± 0.2*	6.6 ± 0.2a	6.8 ± 0.2	5.1 ± 0.4*,b	6.7 ± 0.3	6.2 ± 0.4*
Hemoglobin (g/dl)	14.3 ± 0.3	13.7 ± 0.2	10.7 ± 0.6*,b	13.6 ± 0.5	13.0 ± 0.4*,a	13.3 ± 0.4*	10.2 ± 0.8*,b	13.6 ± 0.5	12.0 ± 0.6*
Hematocrit (%)	41.1 ± 0.8	39.1 ± 1.1	31.3 ± 2.0*,b	38.5 ± 1.3	37.9 ± 1.5*,a	39.0 ± 1.3	29.0 ± 2.4*,b	38.6 ± 1.5	35.6 ± 2.0*
Platelet ($\times 10^3$/μl)	806 ± 42	908 ± 41	1,333 ± 78*,b	920 ± 63	959 ± 65a	929 ± 52	1,105 ± 92*	997 ± 46*	986 ± 65*

All values represent mean ± SEM of $N = 8$–12 animals per group.

G, gestational day.

*$P < 0.05$ compared to BASAL G0.

[a]$P < 0.05$ for DEX G21 vs. CONTROL G21. [b]$P < 0.05$ for G21 vs. G14 in the same group.

week of gestation (**Figure 2b**) was significantly decreased with dexamethasone exposure, but no counteracting effect of bLf nutritional supplementation was found. During the first 2 wk of gestation (G0-G14), food intake was the same in four groups of animals, excluding an impact of bLf supply on this parameter (data not shown). Cumulative food intake during the third week of gestation was significantly reduced in DEX dams (**Figure 2c**). DEX+LACTO dams present a trend to increase their food intake (**Figure 2c**). Food efficiency (weigh gain reported to amount of food intake) was not influenced by bLf but was drastically reduced both in DEX and DEX+LACTO dams (**Figure 2d**).

Since bLf is known to act both as a maturation factor for immune cells and a regulator for iron homeostasis, we analyzed white blood cell content, lymphocyte content, red blood cell content, hemoglobin levels (Hb), hematocrit, and platelet levels in dams (**Table 1**). Measurements were done at gestational day (G) 0, G14 (2 wk following bLf supplementation start/before DEX exposure) and at G21 (3 wk following bLf supplementation start/after 1 wk of DEX exposure). bLf supplementation slightly increased circulating immune cells (without attenuating the immunosuppressive action of DEX) with no effect on hematocrit, red blood cell, and Hb content (**Table 1**).

Litter Characteristics and Body Weight of Offspring at Birth

No difference was observed in the sex ratio of newborn pups within the CONTROL, DEX, and DEX+LACTO litters (**Figure 3a**, inside bar, F = female, M = male). A slight random increase in female proportion ($P = 0.03$) was observed in LACTO litters compared to CONTROL litters. The number of pups per litter was not statistically different in the LACTO group ($P = 0.71$) compared to the CONTROL group. Smaller litters were similarly observed in both the DEX and DEX+LACTO groups ($P < 0.01$ vs. CONTROL; **Figure 3a**). On postnatal day (PND)1, body weight of LACTO pups was significantly higher (≈4%) compared to CONTROL pups ($P < 0.001$; **Figure 3b,c**). As expected, on PND1, weight of DEX pups was decreased compared to respective CONTROL animals ($P < 0.00001$; **Figure 3b,c**). Maternal bLf supplementation during gestation had no effect on DEX-induced IUGR phenotype since PND1 body weight of DEX+LACTO pups were not different to those of respective DEX pups (**Figure 3b,c**). These observations confirm the IUGR phenotype of DEX pups, clearly demonstrate an 4% increase in PND1 weight of pups

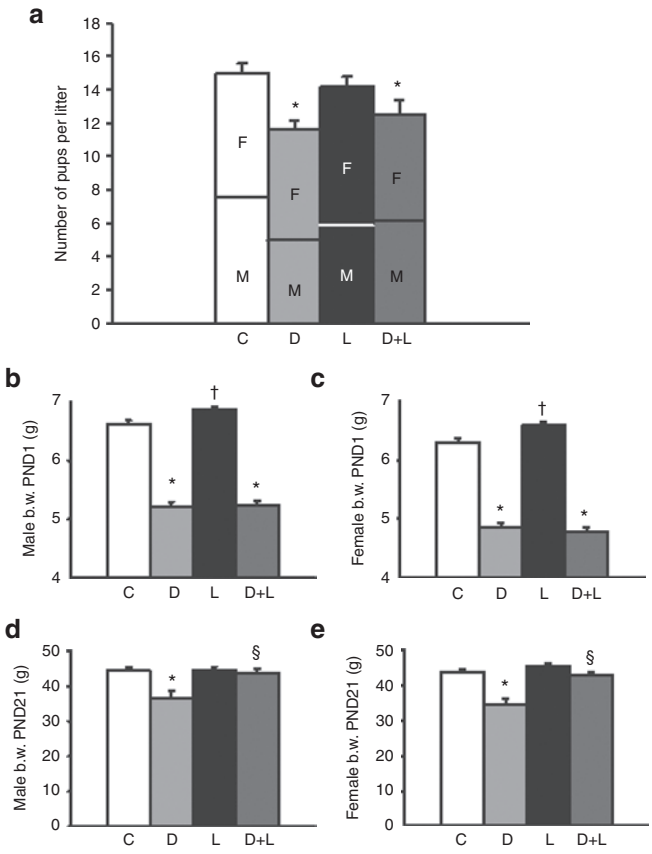

Figure 3. Litter size, sex ratio, and perinatal body weight of pups born to dexamethasone (DEX)-exposed and control dams fed with bLf-enriched or normal diet. (**a**) Number of pups per litter. Results are means ± SEM. N = 16–21 litters per group. *$P < 0.001$ vs. CONTROL. Inside bar: F, female; M, male. The day 1 body weight of (**b**) male and (**c**) female pups. Results are means ± SEM. N = 109–125 pups per group (panel **b**), N = 99–128 pups per group (panel **c**). *$P < 0.001$ vs. CONTROL and †$P < 0.001$ vs. CONTROL. The day 21 body weight (weaning weight) of (**d**) male and (**e**) female pups. Results are means ± SEM. N = 35–60 pups per group (panel **d**), N = 38–45 pups per group (panel **e**). *$P < 0.001$ vs. CONTROL and §$P < 0.001$ vs. DEX. Note the catch-up of DEX+LACTO pups compared to DEX pups in panels **d** and **e**. b.w. body weight; C, CONTROL group (white bar); D, DEX group (light grey bar); D+L, DEX and LACTO group (dark grey bar); L, LACTO group (black bar).

from bLf-supplemented dams, and show no effect of maternal bLf supplementation during gestation on IUGR phenotype of DEX pups at birth.

Early Postnatal Growth of Offspring Until Weaning

Monitoring of pup weight during the lactating period showed that despite initial differences, weight of LACTO pups was similar to that of the respective CONTROL pups at weaning (PND21) (**Figure 3d,e**). DEX pups remain lighter than the respective CONTROL animals ($P < 0.0002$ vs. CONTROL; **Figure 3d,e**). DEX+LACTO animals start a catch-up during the second week of life. At PND21, weight of DEX+LACTO pups was similar to that of the respective CONTROL animals (**Figure 3d,e**), suggesting that maternal nutritional bLf supplementation during lactation allowed to improve the DEX-induced IUGR phenotype.

Neurochemical Profile and Gene Expression in the Hippocampus

We investigated pup hippocampal metabolism and gene expression using both noninvasive *in vivo* approaches (^{1}H NMR spectroscopy) and classical *ex vivo* methods (real-time quantitative PCR and microarray). We focused our attention on the study of hippocampus at PND7 (a significant time point corresponding to a late neuronal proliferative phase) since this brain limbic region involved in the long-term memory process contains high levels of glucocorticoid receptors, making it particularly vulnerable to DEX-induced fetal programming (8,15).

Magnetic resonance imaging showing the voxel of interest used to acquisition of the spectra is illustrated in **Figure 4a**. Interestingly, hippocampal levels of γ-aminobutyric acid ($P < 0.05$), glutamate (Glu) ($P < 0.03$), N-acetylaspartate (NAA) ($P < 0.001$), N-acetylaspartylglutamate (NAAG) ($P < 0.01$), all decreased in DEX-IUGR pups, were partially or fully normalized in DEX+LACTO pups (**Figure 4b**). The same recovery from DEX-altered neurochemical profile through maternal bLf supplementation was observed for hippocampal pools of NAA+NAAG and Glu+Gln (**Figure 4b**). Among the other numerous metabolites consistently quantified from NMR spectra, no change was detected for macromolecules, ascorbate, aspartate, phosphocholine, creatine (Cr), glucose, glutamine, glutathione, inositol, phosphoethanolamine, or taurine (data not shown).

The hippocampal mRNA levels of selected genes involved in neurodevelopment were also assessed on PND7 to corroborate metabolic neurochemistry to specific transcriptional changes. Among the various transcripts screened, brain-derived neurotrophic factor (BDNF) and divalent metal transporter 1 (DMT-1) presented a downexpression in the DEX pups ($P < 0.02$ vs. CONTROL) which is normalized in

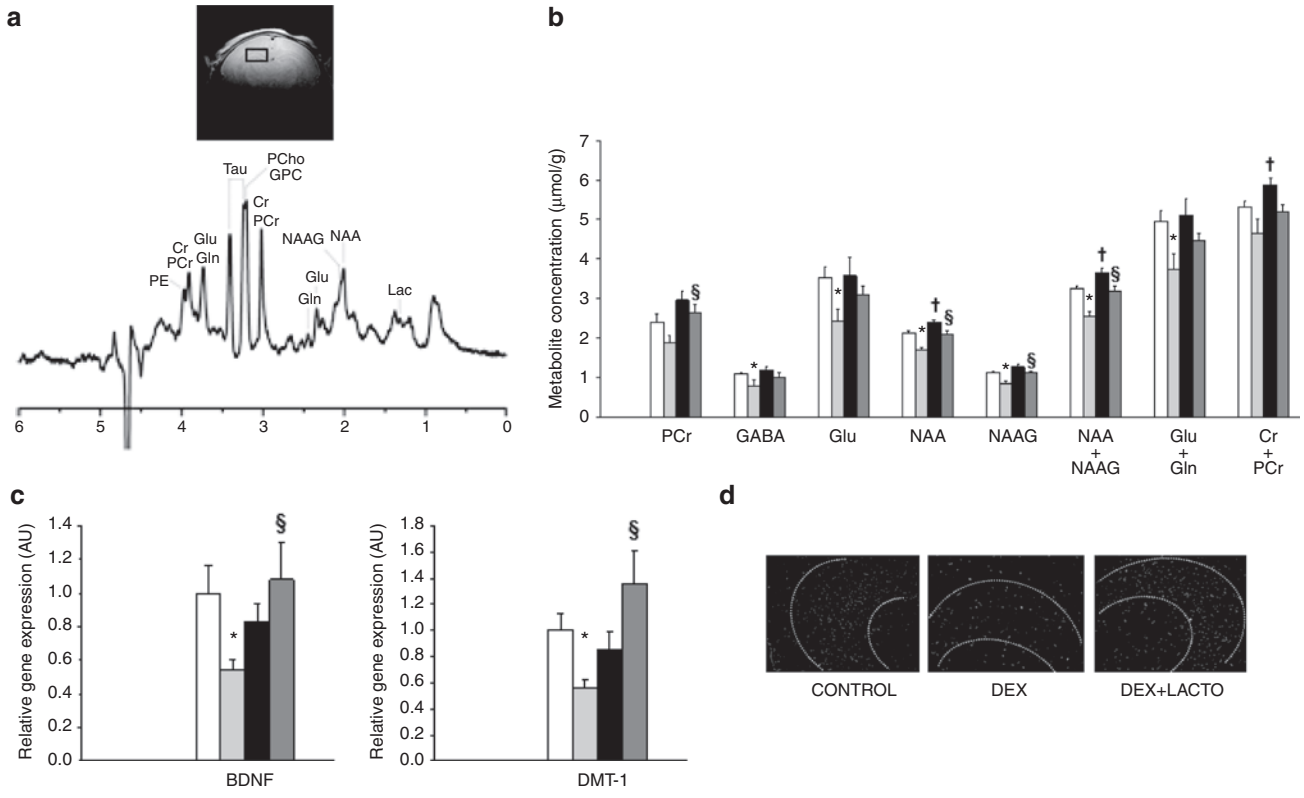

Figure 4. Hippocampus characterization of pups born to dexamethasone (DEX)-exposed and control dams fed with bLf-enriched or normal diet. (**a**) Position of the voxel of interest for hippocampus ^{1}H-MRS and typical spectra of the hippocampus of a CONTROL PND7 pup, (**b**) metabolite concentrations, (**c**) gene expression, and (**d**) representative cell density of the hippocampus at PND7. Results are means ± SEM of $N = 5$–8 pups per group (**b**), $N = 10$ pups per group (**c**). *$P < 0.05$ vs. CONTROL, †$P < 0.05$ vs. CONTROL and §$P < 0.05$ vs. DEX. Abbreviations and color code: C, CONTROL group (white bar); D, DEX group (light grey bar); L, LACTO group (black bar); D+L, DEX and LACTO group (dark grey bar). AU, arbitrary units.

DEX+LACTO pups (**Figure 4c**). Staining of hippocampal slices with 4′-6-Diamidino-2-phenylindole (**Figure 4d**) revealed that molecular and transcriptional changes observed in DEX-IUGR pups lead or reflect a reduced neuronal density. Once again, DEX+LACTO pups appeared similar to CONTROL pups for this endpoint (**Figure 4d**). To further characterize transcriptional changes occurring in the pup developing hippocampus, microarray analyses were performed among the different animal groups. We only considered array gene expression changes greater than 20%, with a P value < 0.001 (**Tables 2** and **3**) and validated some of them by real-time quantitative PCR (**Figure 5**). Transcripts upregulated in DEX pups compared to CONTROL pups belong to the iron-containing oxygen-transport metalloprotein family (Hba-a2, Hbb), to the glutamate signaling and transport pathway (Grm2, Slc1a3) or present neuromodulator functions (Ptgds, Ptn). Gene expression of several transcripts required for a normal cerebral development was downregulated in DEX pups (Plxna2, Ncam1, Dpysl3, Gsk3b, Lsamp, Prkce, Nfix, Crim1, Map1b, Pi4k2a, and Dynlt3). Several neuromodulator transcripts of interest were upregulated in LACTO compared to CONTROL pups: Enc1, Ttr, Plp1, Metrn, Ptma, and Clu. Some of them were also overexpressed in the DEX+LACTO vs. DEX group (Enc1, Metrn, and Ptma). Other transcripts were specifically upregulated in the DEX+LACTO vs. DEX group, such as Nrep, Dhps, and S100b. Transcripts for various glutamate receptors (Grm2, Grin1, and Grin2a) were downregulated in the DEX+LACTO vs. DEX group. Other neuromodulator transcripts present a specific downregulation in the DEX+LACTO vs. DEX group (Dscam, Pard3, and egr1). Gene expression of four genes per comparison (DEX vs. CON (**Figure 5a**), LACTO vs. CON (**Figure 5b**), and DEX+LACTO vs. DEX (**Figure 5c**)) were investigated using real-time quantitative PCR and confirmed a significant change or a clear trend. The correlation between the fold changes observed with the microarray and the real-time quantitative PCR experiment was high, $R = 0.88$, $P < 0.001$ (**Figure 5d**). Together, these observations show that DEX-IUGR hippocampus present specific transcriptional alterations partially reverted with maternal bLf supplementation.

DISCUSSION

In the present study, we evaluated the potentially protective action of bLf, a glycoprotein with pleiotropic actions, on DEX-induced IUGR sequelae, on pup somatic growth and with special focus on brain hippocampus metabolism and gene expression.

The nutritional supplementation with bLf showed no effect on maternal weight gain both during normal and DEX-altered gestation. A gestational window of bLf supplementation also failed to improve the low-birth-weight phenotype of DEX pups but significantly increased by 4% the birth weight of control pups, without any change in litter size, indicating a primary antenatal anabolic action of this nutrient.

Postnatally, DEX-IUGR pups remained lighter than control animals until weaning (PND21), as previously reported (7). Maternal supplementation with bLf during lactation resulted in different effects compared to the gestational period. Despite initial higher birth weights, maternally bLf-exposed pups grew similarly to control pups until PND21. Interestingly, DEX-induced IUGR pups from bLf-supplemented dams started a catch-up growth during the second week of life and showed a total body weight recovery at PND21. Even if underlying mechanisms involved in this catch-up process remain to be elucidated, this observation represents to our knowledge one of the first nutritional intervention able to correct growth in IUGR without overfeeding involving, for example, litter size reduction. Enhanced growth performance has been reported in ICR mice pups from transgenic dams harboring a porcine Lf gene expressed in the mammary gland (16). Maternal bLf supply could act on pup growth, indirectly through dam effects impacting blood or milk composition, or directly following a placental/milk transfer. Some anabolic functions of bLf have previously been reported such as activation of hepatic protein synthesis (17) or improved intestinal function (18). These present rodent observations could be clinically relevant since the highest concentration of Lf is found in colostrum (9) and higher levels of Lf are found in preterm mature milk (19), suggesting a growth-promoting action for Lf during highly sensitive periods of development. Nutritional supplementation with bLf or recombinant Lf could be of great interest to enhance growth in low-birth-weight babies, in addition to its interesting protective effects against sepsis in this frail population (11). The dose presently provided to dams (0.85% w/w in the food pellet) results in a consumption of ~500–1,300 mg bLf/kg of body weight per day, depending on the period (gestation/lactation) considered. This amount is relatively high but provides no supplemental energy intake since it was replaced by isocaloric amount of casein in control food. More work is needed to determine whether bLf presents a dose–response action and whether early bLf exposition allows symmetrical catch-up growth, including a proportional gain of lean, fat, and bone mass. In this sense, the activator effects of bLf on osteoblasts in rodents (20) and the presence of endogenous Lf during the early phases of the human endochondral ossification (21) suggest that Lf harbors a bone-promoting action whereas its effects on adipogenesis remain more elusive (22,23).

Beyond somatic growth, IUGR also impacts brain development, thus increasing the risk for later neurological complications (24). In the present study, we focused our attention on brain hippocampal metabolism and gene expression at PND7, a late neuronal proliferative phase in the rat, documenting for the first time alterations of this tissular development due to DEX-induced IUGR and the potential reversal of these alterations by bLf supplementation. This cerebral part of the limbic system, expressing high levels of glucocorticoid receptors early in life (25) is particularly alterable in the human IUGR situation (5) as well as in DEX-induced IUGR animal models (8,15).

The neurochemical profile detected by high-field ^{1}H NMR spectroscopy (9.4T) allows to noninvasively measure the levels of numerous metabolites reflecting structural

Table 2. Transcriptional upregulations in the developing hippocampus at postnatal day 7

Fold change	Symbol	Definition
		DEX vs. CON (upregulated)
		Iron-containing oxygen-transport metalloprotein family
2.08	LOC287167	Globin, α (LOC287167), mRNA
1.54	MGC72973	β-glo (MGC72973), mRNA
1.51	Eraf	Erythroid-associated factor (predicted), mRNA
1.45	Hba-a2	Hemoglobin α, adult chain 2 (Hba-a2), mRNA
1.42	Hbb	Hemoglobin β chain complex (Hbb), mRNA
1.37	F2r	Coagulation factor II (thrombin) receptor (F2r), mRNA
		Detoxication pathway during drug metabolism
1.62	RGD1561381	Microsomal glutathione S-transferase 3 (predicted), mRNA
1.33	Pex11b	Peroxisomal biogenesis factor 11b (Pex11b), mRNA
1.26	Txnrd1	Thioredoxin reductase 1 (Txnrd1), mRNA
1.24	Ephx2	Epoxide hydrolase 2, cytoplasmic (Ephx2), mRNA
		Glutamate signaling and transport pathway
1.32	Grm2	Glutamate receptor, metabotropic 2 (Grm2), mRNA
1.31	Slc1a3	Glial high-affinity glutamate transporter, member 3 (Slc1a3), mRNA
		Neuromodulator
1.32	Ptn	Pleiotrophin (Ptn), mRNA
1.31	Ptgds	Prostaglandin D2 synthase (brain) (Ptgds), mRNA
1.27	GIPR	Gastric inhibitory polypeptide receptor (Gipr), mRNA
1.23	Vip	Vasoactive intestinal polypeptide (Vip), mRNA
1.20	Rgs4	Regulator of G-protein signaling 4 (Rgs4), mRNA
		Cellular morphology and assembly or reconnaissance pathway
1.38	Gsn	Gelsolin (Gsn), mRNA
1.24	Krt19	Keratin 19 (Krt19), mRNA
1.24	Cadm1	Cell adhesion molecule 1 (Cadm1), mRNA
1.21	Gjb2	Gap junction protein, β 2 (Gjb2), mRNA
1.21	Mrlcb	Myosin light chain, regulatory B (Mrlcb), mRNA
		LACTO vs. CON (upregulated)
		Neuromodulator
1.74	Ptgds	Prostaglandin D2 synthase (brain) (Ptgds), mRNA
1.47	Enc1	Ectodermal-neural cortex 1 (Enc1), mRNA
1.23	Ptma	Prothymosin α (Ptma), mRNA
1.23	Metrn	Meteorin, glial cell differentiation regulator (Metrn), mRNA
1.23	Clu	Clusterin (Clu), mRNA
1.23	Id2	Inhibitor of DNA binding 2 (Id2), mRNA
		Cellular morphology and assembly or reconnaissance pathway
1.51	Eml2	Echinoderm microtubule associated protein like 2 (Eml2), mRNA
1.30	Necab2	N-terminal EF-hand calcium binding protein 2 (Necab2), mRNA
1.27	Tpm4	Tropomyosin 4 (Tpm4), mRNA
1.27	Cldn5	Claudin 5 (Cldn5), mRNA
1.26	Plp1	Proteolipid protein 1 (Plp1), mRNA
1.23	Tagln2	Transgelin 2 (Tagln2), mRNA
1.21	Tm7sf2	Transmembrane 7 superfamily member 2 (Tm7sf2), mRNA
1.20	Asb2	Ankyrin repeat and SOCS box-containing 2 (Asb2), mRNA
1.20	Pigy	Phosphatidylinositol glycan anchor biosynthesis, class Y (Pigy), mRNA
1.20	Tuba4a	Tubulin, α 4A (Tuba4a), mRNA
		Nutritional marker
1.28	Ttr	Transthyretin (Ttr), mRNA
1.23	Alb	Albumin (Alb), mRNA
		DEX+LACTO vs. DEX (upregulated)
		Neuromodulator
1.45	Enc1	Ectodermal-neural cortex 1 (Enc1), mRNA
1.30	Metrn	Meteorin, glial cell differentiation regulator (Metrn), mRNA
1.26	Ptma	Prothymosin α (Ptma), mRNA
1.24	Nrep	Neuronal regeneration related protein (Nrep), mRNA
1.23	S100b	S100 calcium binding protein B (S100b), mRNA
1.21	Dhps	Deoxyhypusine synthase (Dhps), mRNA
		Cellular morphology and assembly or reconnaissance pathway
1.41	LOC689827	Myosin-9B (myosin IXb) (unconventional myosin-9b), mRNA
1.41	Argbp2	Arg/Abl-interacting protein ArgBP2 (Argbp2), mRNA
1.28	Dynlrb2	Dynein light chain roadblock-type 2 (predicted), mRNA
1.27	Dnah1	Dynein, axonemal, heavy chain 1 (Dnah1), mRNA
1.25	Canx	Calnexin (Canx), mRNA
1.23	Tpm4	Tropomyosin 4 (Tpm4), mRNA
1.21	Ctnnb1	Catenin (cadherin associated protein), β 1 (Ctnnb1), mRNA
1.21	Tekt1	Tektin 1 (Tekt1), mRNA

Table 3. Transcriptional downregulations in the developing hippocampus at PND7

Fold change	Symbol	Definition
		DEX vs. CON (downregulated)
		Cell migration/axonal guidance/neurite outgrowth
0.81	Ncam1	Neural cell adhesion molecule 1 (Ncam1), mRNA
0.80	Plxna2	Plexin A2 (predicted), mRNA
0.80	Gsk3b	Glycogen synthase kinase 3 β (Gsk3b), mRNA
0.78	Lsamp	Limbic system-associated membrane protein (Lsamp), mRNA
0.75	Prkce	Protein kinase C, epsilon (Prkce), mRNA
0.72	Dpysl3	Dihydropyrimidinase-like 3 (Dpysl3), mRNA
		Neuromodulator
0.79	Crim1	Cysteine-rich motor neuron 1 (predicted), mRNA
0.78	Appbp2	Amyloid β precursor protein binding protein 2 (Appbp2), mRNA
0.76	Nfix	Nuclear factor I/X (Nfix), mRNA
0.72	Cnr1	Cannabinoid receptor 1 (brain) (Cnr1), mRNA
		Cellular morphology and assembly or reconnaissance pathway
0.78	Pi4k2a	Phosphatidylinositol 4-kinase type 2 α (Pi4k2a), mRNA
0.73	Map1b	Microtubule-associated protein 1b (Map1b), mRNA
0.72	Dynlt3	Dynein light chain Tctex-type 3 (Dynlt3), mRNA
0.70	Plekhf2	Pleckstrin homology domain containing, family F member 2 (predicted), mRNA
0.70	Argbp2	Arg/Abl-interacting protein ArgBP2 (Argbp2), mRNA
		LACTO vs. CON (downregulated)
		Gene expression regulator
0.79	Bat1	HLA-B associated transcript 1 (Bat1), mRNA
0.76	Hdac4	Histone deacetylase 4 (predicted), mRNA
0.73	Hdac5	Histone deacetylase 5 (Hdac5), mRNA
		Thyroid metabolism
0.65	Thrb	Thyroid hormone receptor β (Thrb), mRNA
		DEX+LACTO vs. DEX (downregulated)
		Thyroid metabolism
0.76	Klf9	Kruppel-like factor 9 (Klf9), mRNA
0.61	Thrb	Thyroid hormone receptor β (Thrb), mRNA
		Detoxication pathway during drug metabolism
0.64	Ephx2	Epoxide hydrolase 2, cytoplasmic (Ephx2), mRNA
0.44	RGD1561381	Microsomal glutathione S-transferase 3 (predicted), mRNA
		Glutamate signaling and transport pathway
0.81	Grin2a	Glutamate receptor, ionotropic, N-methyl D-aspartate 2A (Grin2a), mRNA
0.80	Grin1	Glutamate receptor, ionotropic, N-methyl D-aspartate 1 (Grin1), mRNA
0.79	Slc1a3	Glial high affinity glutamate transporter, member 3 (Slc1a3), mRNA
0.78	Grm2	Glutamate receptor, metabotropic 2 (Grm2), mRNA
		Neuromodulator
0.81	Dscam	Down syndrome cell adhesion molecule (Dscam), mRNA
0.81	Pard3	Par-3 (partitioning defective 3) homolog (*Caenorhabditis elegans*) (Pard3), mRNA
0.80	Gm2a	GM2 ganglioside activator (Gm2a), mRNA
0.80	Egr1	Early growth response 1 (Egr1), mRNA
0.80	Synj2	Synaptojanin 2 (Synj2), mRNA
0.55	Dnmt3a	DNA methyltransferase 3A (Dnmt3a), transcript variant 2, mRNA
		Cellular morphology and assembly or reconnaissance pathway
0.81	Itga1	Integrin α 1 (Itga1), mRNA
0.81	Actg2	Actin, gamma 2, smooth muscle, enteric (Actg2), mRNA
0.80	Lgals5	Lectin, galactose binding, soluble 5 (Lgals5), mRNA
0.80	Mmp14	Matrix metallopeptidase 14 (membrane-inserted) (Mmp14), mRNA
0.80	Notch1	Notch gene homolog 1 (*Drosophila*) (Notch1), mRNA
0.80	Col3a1	Collagen, type III, α 1 (Col3a1), mRNA
0.77	Dync1li1	Dynein cytoplasmic 1 light intermediate chain 1 (Dync1li1), mRNA
0.77	Gjb6	Gap junction protein, β 6 (Gjb6), mRNA
0.76	Tagln	Transgelin (Tagln), mRNA
0.76	Pkp2	Plakophilin 2 (Pkp2), mRNA
0.75	Gsn	Gelsolin (Gsn), mRNA
0.75	Lox	Lysyl oxidase (Lox), mRNA
0.70	Myo5a	Myosin Va (Myo5a), mRNA

and functional characteristics of selected cerebral regions. Interestingly, we observed that hippocampal levels of excitatory (glutamate) and inhibitory (γ-aminobutyric acid) neurotransmitters and neuronal markers (NAA) were significantly decreased in DEX-induced IUGR pups and were partially or fully normalized with maternal bLf supply. BDNF gene expression strikingly followed the same regulation pattern. These results, corroborated by our histological observations, suggest that neuronal density in the hippocampus is dampened in DEX-induced IUGR pups but normalized with maternal bLf supply. Previous studies also report BDNF downregulation by synthetic corticoids. *In vivo*, direct

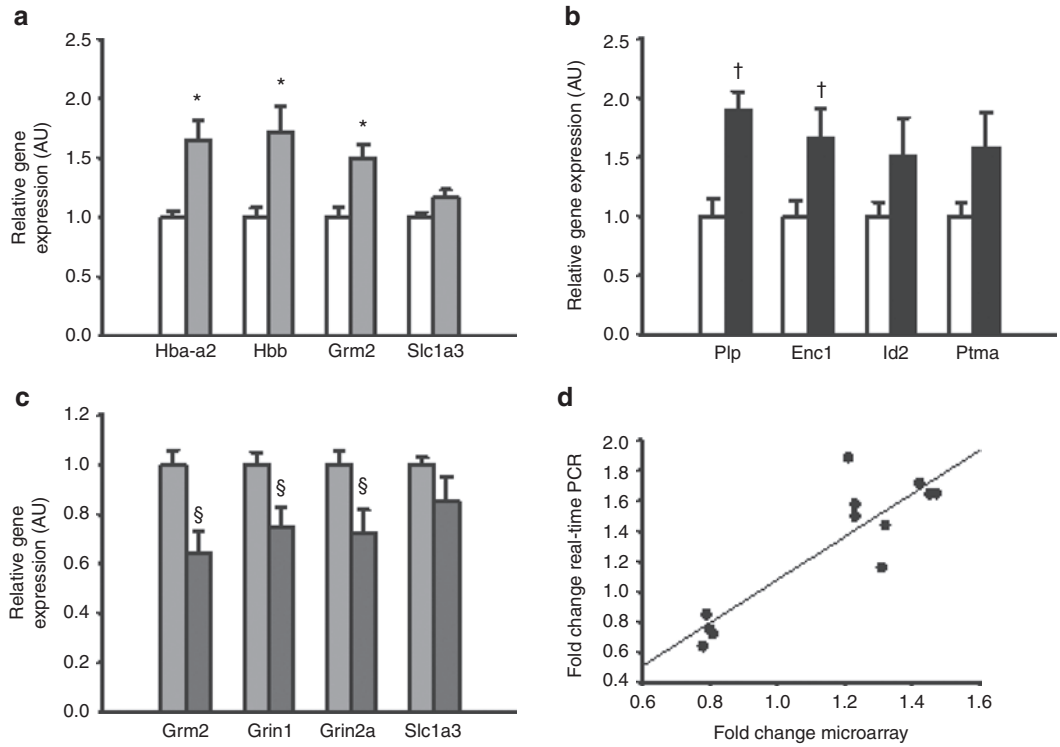

Figure 5. Validation of microarray gene expression changes using real-time quantitative PCR. Hippocampus mRNA levels of selected genes (**a**) in CONTROL and DEX pups, (**b**) in CONTROL and LACTO pups, (**c**) in DEX and DEX+LACTO pups at postnatal day 7. For all panels, relative results obtained by real-time qPCR are expressed in arbitrary units (AU) and each bar represents the mean ± SEM of $n = 10$ animals per group. $^{*}P < 0.05$ vs. CONTROL, $^{\dagger}P < 0.05$ vs. CONTROL and $^{\S}P < 0.05$ vs. DEX. (**d**) Linear regression analysis of fold-change from microarray and real-time qPCR results. Correlation coefficient $R = 0.88$, $P < 0.001$. Enc1, ectodermal-neural cortex 1; Grin1, glutamate receptor ionotropic N-methyl D-aspartate 1; Grin2a, glutamate receptor ionotropic N-methyl D-aspartate 2A; Grm2, glutamate receptor metabotropic 2; Hba-a2, hemoglobin α adult chain 2; Hbb, hemoglobin β chain complex; Id2, inhibitor of DNA binding 2; Slc1a3, glial high affinity glutamate transporter; Ptma, prothymosin α; Plp1, proteolipid protein 1.

exposure to dexamethasone was reported to decrease the level of BDNF mRNA in the rat hippocampus (26), and prenatal dexamethasone exposure blocks the stimulated BDNF elevation in the paraventricular nucleus (27). In the same way, *in vitro*, dexamethasone prevents activity-dependent increases in BDNF in rat hippocampal neurons (28) through different mechanisms including (i) inhibition of postsynaptic $Ca^{(2+)}$ influx (29), (ii) inhibition of presynaptic glutamate release (29) via a direct glucocorticoid receptor-BDNF receptor interaction (30), and (iii) blockade of the signaling pathway mediating the BDNF-induced synaptic proteins involved in neuron maturation (29). Both these data and our present results suggest that in DEX-induced IUGR pup hippocampus, decreased levels of BDNF and glutamate could potentiate each other leading to limitation in neuronal development. Another cross-observation between ^{1}H NMR spectroscopy results and transcriptomic approaches was illustrated by decreased hippocampal levels of NAAG (a neuromodulatory peptide expressed in neuronal terminals) associated with overexpression of the presynaptic glutamate receptor metabotropic 2 (Grm2) in DEX-IUGR pups. NAAG is known to bind both presynaptic metabotropic glutamate receptors Grm2/3 to limit neurotransmitter release (31) and postsynaptic N-methyl-D-aspartate receptors with agonistic (32) or antagonistic activity (33). Once again, hippocampal levels of NAAG, Grm2 mRNA as well as N-methyl-D-aspartate receptor subunits 1 (Grin1) and 2A (Grin2a) mRNA were normalized with maternal bLf supplementation. N-methyl-D-aspartate receptors are centrally involved in hippocampal synaptic plasticity (34) and seem to be selectively targeted in the IUGR situation. Altered composition of glutamate receptor subunits was recently observed in the hippocampus of IUGR rats born from an uteroplacental insufficiency model (35) and N-methyl-D-aspartate receptor subtype 2B (Grin2b) was increased in the hippocampus of prenatally stressed rats (36).

Microarrays allowed us to deeper characterize the hippocampal transcriptomic hallmark in DEX-IUGR pups as well as the impact of maternal bLf. As very subtle transcriptional responses are generally observed in the brain following experimental interventions, we considered biologically relevant and statistically significant gene expression changes greater than 20%, with a P value < 0.001. We also validated some microarray observations using real-time quantitative PCR. The correlation between the fold changes observed with the microarray and with the real-time quantitative PCR method was high ($R = 0.88$; $P < 0.001$) although this relation is known to become weaker with changes below 1.5-fold (37). Numerous transcripts identified in the literature as required for normal cerebral development were downregulated in our

IUGR model, interfering in cell migration, axonal guidance, or neurite outgrowth. Some of them are of particular interest, such as Plxna2 (a semaphorin receptor), Map1b (a microtubule bundle formation molecule), Dpysl3 (a key player in axonal growth), Gsk3b (a kinase mediating neurogenesis and neuronal polarization), Lsamp (a recognition molecule for the formation of limbic connections), Prkce (a kinase with a role in neurite outgrowth and presynaptic regulation), Nfix (a transcription factor required for neural stem cell homeostasis), and Crim1 (a growth factor binding transmembrane protein). Conversely, the highest upregulated transcripts in the DEX-IUGR hippocampus were the iron-containing oxygen-transport metalloproteins (Hba-a2 and Hbb). This "ectopic" expression, out of red blood cells, corroborates recent neuronal hemoglobin detection with an oxygen capacitator activity (38).

It was also interesting to note that some transcripts of interest were upregulated in control pups born to bLf-supplemented dams, such as Ttr (a transport protein for retinol-binding protein/thyroxine, widely used as a clinical nutritional marker), Plp1 (a protein associated with myelin biogenesis/compaction), Metrn (a neurotrophic factor), Ptma (a necrosis inhibitor) and Clu (a glycoprotein chaperone molecule). This transcriptional effect of maternal bLf-supply in normal conditions was associated with increased levels of NAA and pools of NAA+NAAG and Cr+PCr. Other transcripts were specifically upregulated by maternal bLf exclusively in DEX-IUGR pups, such as Nrep (neuronal regeneration related protein) and S100b (a marker of the nervous system damage at adulthood with neurotrophic function in the developping central nervous system and shown as decreased following prenatal stress) (39).

We observed no difference in maternal red blood cell, Hb, or hematocrit levels in response to bLf supply, as previously reported after long-term delivery of 200–2,000 mg bLf/kg/d (40) or 1,800 mg recombinant human apo-Lf/kg/d (41) in adult rats. Together, these results confirm that the bLf supplementation does not interfere with maternal hematocrit during normal iron availability in rats in contrast to its antianemic action described in recent clinical studies (42). Benefits of maternal bLf supplementation on DEX pups do not appear to be directly mediated by an improved maternal iron metabolism. However, hippocampal gene expression of DMT-1 (a cellular iron/metal transporter from the plasma membrane to endosomes), decreased in IUGR pups was restored with maternal bLf-supply, suggesting that more investigations in the field of pup hippocampal iron metabolism are required. DMT-1 is expressed in various cerebral cell types suggesting an important role in metal homeostasis in the brain (43). Moreover, a specific knock-out mouse model has shown that neuronal iron uptake by DMT-1 is essential for normal hippocampal neuronal development (44). Iron availability was shown to impact the neurochemical profile, apical dendritic growth, maturation of synaptic function, and gene expression in the developing hippocampus (for review, see ref. 45).

Taken together, our present observations demonstrate for the first time that maternal supplementation with bLf stimulates fetal growth in normal gestation and allows DEX-induced IUGR pups to catch-up during the lactating period. Hippocampal altered metabolites and gene expression are hallmarks of DEX-induced IUGR changes. These alterations may indicate defective hippocampal development resulting in later cognitive impairment. In reversing several of the DEX-induced IUGR sequelae, maternal bLf supplementation could be viewed as a promising nutritional intervention for early neuroprotection and growth support.

METHODS

Animal Care and Diets

All experimental protocols were approved by the State of Geneva Veterinary Office (Geneva, Switzerland). Pregnant Sprague Dawley OFA rat dams (Charles River Laboratories, L'Arbresle, France) were housed individually under standard conditions (Faculty of Medicine, Geneva University) with free access to either normal or bLf-enriched diet. Both diets, strictly isocaloric and prepared in Nestlé Research Center (Vers-chez-les-Blanc, Switzerland), contain 52% cornstarch, 10% sucrose, 7% soybean oil, 5% cellulose, 3.5% mineral mix AIN-93G, 1% vitamin mix AIN-93, 0.25% choline bitartrate, 0.3% L-cystine, and 0.0014% Tert-butylhydroquinone. Control diet contains 20.85% casein whereas bLf-enriched diet contains 20% casein and 0.85% bLf. Iron content in bLf supply is 120 ppm, representing a negligeable contribution to whole food iron content. Estimated bLf consumption ranges from ~500 mg (during gestation) to 1,300 mg (during lactation) bLf/kg of body weight. Weight and food intake of dams were monitored weekly during gestation and pups weights were monitored weekly until weaning. At PND1, litter size was brought to 10–12 pups per dam to avoid any confounding litter size effect.

DEX Exposure

Control and bLf-fed dams were implanted subcutaneously with an Alzet osmotic minipump (Charles River Laboratories) delivering either vehicle or dexamethasone at the dose of 100 µg/kg/d (Sigma-Aldrich, Buchs, Switzerland) from gestational day 14 to 21.

Hematological Measurements

Maternal blood was collected in EDTA-coated tubes on G0 (just before food group assignation), on G14 (2 wk after initiation of bLf-enriched or normal diet consumption), and on G21 (after 1 wk of subcutaneous dexamethasone or vehicle exposure). Hematological values were obtained using an automated hematology analyzer KX-21 (Sysmex Europe, Norderstedt, Deutschland).

In Vivo ^{1}H NMR Spectroscopy

In vivo ^{1}H MRS was performed on PND7 pups under isoflurane (1.5–2%) using a 9.4T/31 cm magnet (Magnex Scientific, Abington, UK; Varian, Palo Alto, CA) equipped with 12-cm gradient coils (400 mT/m, 120 µs). A transceive 17-mm-diameter ^{1}H quadrature surface coil was used. A voxel of interest ($1.5 \times 2.5 \times 2.5\,mm^3$) was placed in the hippocampus. First- and second-order shims were adjusted using fast automatic shimming technique by mapping along projections. Spectra were acquired using an ultra-short echo time SPECIAL spectroscopy method with TE/TR = 2.7/4,000 ms and 30 blocks of 16 averages. The metabolite concentrations were quantified using LCModel. The water spectra were used as reference assuming cerebral water content of 87.8% at PND7. The results provided the quantification of the following 17 metabolite concentrations in the hippocampus: macromolecules, ascorbate, β-hydroxybutyrate, phosphorylcholine, creatine, phosphocreatine, γ-aminobutyric acid, glucose, glutamate, glutamine, myoinositol, lactate, N-acetylaspartate, N-acetylaspartylglutamate, phosphocreatine, phosphoethanolamine, and taurine.

Microarray Analysis

At PND7, the hippocampus from 10 pups originating from three independent litters for each group were carefully dissected, frozen in liquid nitrogen, and stored at −80 °C before being disrupted

Table 4. PCR primers for quantitative real-time PCR

	Forward	Reverse
Bdnf	5′-AAAAAGTTCCACCAGGTGAGAAGA-3′	5′-GCAACCGAAGTATGAAATAACCATAG-3′
Dmt1	5′-GATCATGCCACACAACATGTACCT-3′	5′-TTCTCGAACTTCCTGCTTATTGG-3′
Hba-a2	5′-TGCGTGTGGATCCTGTCAA-3′	5′-GTGGTGGCAAGCCAAGGT-3′
Hbb	5′-GACAAGCTGCATGTGGATCCT-3′	5′-TGGCCCAACACAATCACAAT-3′
Grm2	5′-CCATCCAGGTGGCCAATCT-3′	5′-GGTGGAGGCATAGCTGATCTG-3′
Slc1a3	5′-CATTGGAGGGTTGCTGCAA-3′	5′-GCAGGGTGGCAGAACTTGAG-3′
Plp	5′-TCATTAATGTGATTCATGCTTTCCA-3′	5′-GCCCCATAAAGGAAGAAGAAAGA-3′
Enc1	5′-CGCCACTACTGAGTTGAAACAAA-3′	5′-CCCTGGACTTGCGGTTCTC-3′
Id2	5′-CCGCTGACCACCCTGAAC-3′	5′-AATTCAGACGCCTGCAAGGA-3′
Ptma	5′-GGACACCAGCTCCGAGATCA-3′	5′-CCTCCTCCACAACTTCCTTCTTC-3′
Grin1	5′- CATCTGGAAGACAGGACCATTG-3′	5′-CACTCCGTCCGCATACTTAGAA-3′
Grin2a	5′-TCACAGGCGTGTGCTCTGA-3′	5′-AACTATAGATGCCCCTGCTGATG-3′
RPS29	5′-GCCAGGGTTCTCGCTCTTG-3′	5′-GGCACATGTTCAGCCCGTAT-3′
Tubulin	5′-GCAGTGCGGCAACCAGAT-3′	5′-AGTGGGATCAATGCCATGCT-3′

and homogenized in lysis buffer using FastPrep instrument/lysing tubes containing ceramic beads (MP Biomedicals Europe, Illkirch, France). Total RNA was then extracted, purified with the RNAdvance Agencourt tissue kit (Beckman Coulter, Nyon, Switzerland) with a Hamilton robotic station (Hamilton, Bonaduz, Switzerland). RNA was quantified with the RiboGreen RNA Quantification Kit (MP Biomedicals Europe) and monitored for quality on an Agilent 2100 Bioanalyser (Agilent Technologies, Morges, Switzerland). cRNA targets were synthesized, labeled, and purified according to the Illumina TotalPrep RNA amplification protocol (Illumina, San Diego, CA). Hybridization mix was applied to each microarray (RatRef-12 Expression BeadChips; Illumina). After hybridization (16 h, 58 °C), the microarrays were washed, stained with Streptavidin-Cy3 and scanned with a BeadArray Reader (Illumina). Signal intensities were extracted and summarized in the GenomeStudio software (Illumina). Data were expressed as absolute intensities. Quality control of the data was performed on all samples with a Pearson correlation matrix and a principal component analysis. After $\log_2$ transformation, data were quantile normalized and analyzed by ANOVA, followed by a Global Error Assessment. Gene expression changes greater than 20% with a P value < 0.001 were considered as biologically relevant and statistically significant.

Real-Time Quantitative PCR

Two micrograms of total RNA were reverse transcribed using 400 units of Moloney murine leukemia virus reverse transcriptase (Invitrogen, Basel, Switzerland), 1 unit/µl RNAsin (Promega, Madison, WI), 0.2 µg of random primers (oligo(dN)6) (Promega), 2 mmol/l dNTP, and 20 µmol/l of dithiothreitol (Invitrogen). Gene expression of the cDNAs of interest was determined by real-time quantitative PCR using an ABI StepOne Plus Sequence Detection System (Applera Europe, Rotkreuz, Switzerland) and were normalized using the housekeeping gene RPS29 or tubulin. List of primers is provided in **Table 4**.

Histology

At PND7, pups were anesthetized, perfused intracardially with 0.9% NaCl and then with 4% paraformaldehyde. Brains were removed, postfixed in 4% paraformaldehyde overnight, then 30% sucrose for 24 h and stored at −80°C. Ten micrometer sections at the level of the hippocampus were classically cut on a cryostat before being blocked with 4% BSA (Sigma-Aldrich), then with 0.3% Triton/PBS 1X for 60 min and incubated with 4′-6-diamidino-2-phenylindole. Digital images were obtained using a microscope coupled with a camera AxioCam MRc5 controlled by Axiovision AC software (Carl Zeiss MicroImaging GmbH, Germany).

Statistics

Animals originated from at least three independent litters in each group for each endpoint investigated to account for the intragroup variability between litters. Results are expressed as mean ± SEM. We performed the unpaired Student's t-test and repeated-measures one-way ANOVA. We considered a P value of < 0.05 as statistically significant.

ACKNOWLEDGMENTS

We acknowledge the excellent technical assistance of Noëlle Greco and the whole team of the Maternité-Pédiatrie laboratory for the hematological measurements. We are grateful to M.L. Aubert for advice concerning the manuscript.

REFERENCES

1. World health statistics report 2012. http://www.who.int/gho/publications/world_health_statistics/EN_WHS2012_Fullpdf.
2. Barker DJ, Eriksson JG, Forsén T, Osmond C. Fetal origins of adult disease: strength of effects and biological basis. Int J Epidemiol 2002;31:1235–9.
3. Latal-Hajnal B, von Siebenthal K, Kovari H, Bucher HU, Largo RH. Postnatal growth in VLBW infants: significant association with neurodevelopmental outcome. J Pediatr 2003;143:163–70.
4. Mallard C, Loeliger M, Copolov D, Rees S. Reduced number of neurons in the hippocampus and the cerebellum in the postnatal guinea-pig following intrauterine growth-restriction. Neuroscience 2000;100:327–33.
5. Lodygensky GA, Seghier ML, Warfield SK, et al. Intrauterine growth restriction affects the preterm infant's hippocampus. Pediatr Res 2008;63:438–43.
6. Modi N, Lewis H, Al-Naqeeb N, Ajayi-Obe M, Doré CJ, Rutherford M. The effects of repeated antenatal glucocorticoid therapy on the developing brain. Pediatr Res 2001;50:581–5.
7. Somm E, Vauthay DM, Guérardel A, et al. Early metabolic defects in dexamethasone-exposed and undernourished intrauterine growth restricted rats. PLoS ONE 2012;7:e50131.
8. Noorlander CW, Visser GH, Ramakers GM, Nikkels PG, de Graan PN. Prenatal corticosteroid exposure affects hippocampal plasticity and reduces lifespan. Dev Neurobiol 2008;68:237–46.
9. Nagasawa T, Kiyosawa I, Kuwahara K. Amounts of lactoferrin in human colostrum and milk. J Dairy Sci 1972;55:1651–9.
10. García-Montoya IA, Cendón TS, Arévalo-Gallegos S, Rascón-Cruz Q. Lactoferrin a multiple bioactive protein: an overview. Biochim Biophys Acta 2012;1820:226–36.
11. Manzoni P, Rinaldi M, Cattani S, et al.; Italian Task Force for the Study and Prevention of Neonatal Fungal Infections, Italian Society of Neonatology.

Bovine lactoferrin supplementation for prevention of late-onset sepsis in very low-birth-weight neonates: a randomized trial. JAMA 2009;302:1421–8.
12. Fillebeen C, Dexter D, Mitchell V, et al. Lactoferrin is synthesized by mouse brain tissue and its expression is enhanced after MPTP treatment. Adv Exp Med Biol 1998;443:293–300.
13. An L, Sato H, Konishi Y, et al. Expression and localization of lactotransferrin messenger RNA in the cortex of Alzheimer's disease. Neurosci Lett 2009;452:277–80.
14. Ji B, Maeda J, Higuchi M, et al. Pharmacokinetics and brain uptake of lactoferrin in rats. Life Sci 2006;78:851–5.
15. Uno H, Lohmiller L, Thieme C, et al. Brain damage induced by prenatal exposure to dexamethasone in fetal rhesus macaques. I. Hippocampus. Brain Res Dev Brain Res 1990;53:157–67.
16. Wu SC, Chen HL, Yen CC, et al. Recombinant porcine lactoferrin expressed in the milk of transgenic mice enhances offspring growth performance. J Agric Food Chem 2007;55:4670–7.
17. Burrin DG, Wang H, Heath J, Dudley MA. Orally administered lactoferrin increases hepatic protein synthesis in formula-fed newborn pigs. Pediatr Res 1996;40:72–6.
18. Liao Y, Jiang R, Lönnerdal B. Biochemical and molecular impacts of lactoferrin on small intestinal growth and development during early life. Biochem Cell Biol 2012;90:476–84.
19. Ronayne de Ferrer PA, Baroni A, Sambucetti ME, Lopez NE, Ceriani Cernadas JM. Lactoferrin levels in term and preterm milk. J Am Coll Nutr 2000;19:370–3.
20. Cornish J, Callon KE, Naot D, et al. Lactoferrin is a potent regulator of bone cell activity and increases bone formation in vivo. Endocrinology 2004;145:4366–74.
21. Antonio I, Valeria B, Maddalena G, Giovanni T. Immunohistochemical evidence of lactoferrin in human embryo-fetal bone and cartilage tissues. Cell Biol Int 2010;34:845–9.
22. Moreno-Navarrete JM, Ortega FJ, Ricart W, Fernandez-Real JM. Lactoferrin increases (172Thr)AMPK phosphorylation and insulin-induced (p473Ser)AKT while impairing adipocyte differentiation. Int J Obes (Lond) 2009;33:991–1000.
23. Moreno-Navarrete JM, Ortega F, Sabater M, Ricart W, Fernández-Real JM. Proadipogenic effects of lactoferrin in human subcutaneous and visceral preadipocytes. J Nutr Biochem 2011;22:1143–9.
24. Saigal S, Pinelli J, Hoult L, Kim MM, Boyle M. Psychopathology and social competencies of adolescents who were extremely low birth weight. Pediatrics 2003;111(5 Pt 1):969–75.
25. Yi SJ, Masters JN, Baram TZ. Glucocorticoid receptor mRNA ontogeny in the fetal and postnatal rat forebrain. Mol Cell Neurosci 1994;5:385–93.
26. Barbany G, Persson H. Regulation of Neurotrophin mRNA Expression in the Rat Brain by Glucocorticoids. Eur J Neurosci 1992;4:396–403.
27. Hossain A, Hajman K, Charitidi K, et al. Prenatal dexamethasone impairs behavior and the activation of the BDNF exon IV promoter in the paraventricular nucleus in adult offspring. Endocrinology 2008;149:6356–65.
28. Cosi C, Spoerri PE, Comelli MC, Guidolin D, Skaper SD. Glucocorticoids depress activity-dependent expression of BDNF mRNA in hippocampal neurones. Neuroreport 1993;4:527–30.
29. Kumamaru E, Numakawa T, Adachi N, et al. Glucocorticoid prevents brain-derived neurotrophic factor-mediated maturation of synaptic function in developing hippocampal neurons through reduction in the activity of mitogen-activated protein kinase. Mol Endocrinol 2008;22:546–58.
30. Numakawa T, Kumamaru E, Adachi N, Yagasaki Y, Izumi A, Kunugi H. Glucocorticoid receptor interaction with TrkB promotes BDNF-triggered PLC-gamma signaling for glutamate release via a glutamate transporter. Proc Natl Acad Sci USA 2009;106:647–52.
31. Zhao J, Ramadan E, Cappiello M, Wroblewska B, Bzdega T, Neale JH. NAAG inhibits KCl-induced [(3)H]-GABA release via mGluR3, cAMP, PKA and L-type calcium conductance. Eur J Neurosci 2001;13:340–6.
32. Westbrook GL, Mayer ML, Namboodiri MA, Neale JH. High concentrations of N-acetylaspartylglutamate (NAAG) selectively activate NMDA receptors on mouse spinal cord neurons in cell culture. J Neurosci 1986;6:3385–92.
33. Bergeron R, Imamura Y, Frangioni JV, Greene RW, Coyle JT. Endogenous N-acetylaspartylglutamate reduced NMDA receptor-dependent current neurotransmission in the CA1 area of the hippocampus. J Neurochem 2007;100:346–57.
34. Bliss TV, Collingridge GL. A synaptic model of memory: long-term potentiation in the hippocampus. Nature 1993;361:31–9.
35. Schober ME, McKnight RA, Yu X, Callaway CW, Ke X, Lane RH. Intrauterine growth restriction due to uteroplacental insufficiency decreased white matter and altered NMDAR subunit composition in juvenile rat hippocampi. Am J Physiol Regul Integr Comp Physiol 2009;296:R681–92.
36. Neeley EW, Berger R, Koenig JI, Leonard S. Strain dependent effects of prenatal stress on gene expression in the rat hippocampus. Physiol Behav 2011;104:334–9.
37. Dallas PB, Gottardo NG, Firth MJ, et al. Gene expression levels assessed by oligonucleotide microarray analysis and quantitative real-time RT-PCR – how well do they correlate? BMC Genomics 2005;6:59.
38. Schelshorn DW, Schneider A, Kuschinsky W, et al. Expression of hemoglobin in rodent neurons. J Cereb Blood Flow Metab 2009;29:585–95.
39. Van den Hove DL, Steinbusch HW, Bruschettini M, et al. Prenatal stress reduces S100B in the neonatal rat hippocampus. Neuroreport 2006;17:1077–80.
40. Yamauchi K, Toida T, Nishimura S, et al. 13-Week oral repeated administration toxicity study of bovine lactoferrin in rats. Food Chem Toxicol 2000;38:503–12.
41. Cerven D, DeGeorge G, Bethell D. 28-day repeated dose oral toxicity of recombinant human holo-lactoferrin in rats. Regul Toxicol Pharmacol 2008;52:174–9.
42. Paesano R, Torcia F, Berlutti F, et al. Oral administration of lactoferrin increases hemoglobin and total serum iron in pregnant women. Biochem Cell Biol 2006;84:377–80.
43. Williams K, Wilson MA, Bressler J. Regulation and developmental expression of the divalent metal-ion transporter in the rat brain. Cell Mol Biol (Noisy-le-grand) 2000;46:563–71.
44. Carlson ES, Tkac I, Magid R, et al. Iron is essential for neuron development and memory function in mouse hippocampus. J Nutr 2009;139:672–9.
45. Georgieff MK. The role of iron in neurodevelopment: fetal iron deficiency and the developing hippocampus. Biochem Soc Trans 2008;36(Pt 6):1267–71.